Electronic Supplementary Material (ESI) for ChemComm.

Supporting Information

High acetylene/ethylene separation in a microporous zinc(II) metal–organic framework with low binding energy

Hui-Min Wen,[a] Bin Li,*[a] Hailong Wang,[a] Rajamani Krishna,[b] and Banglin Chen*[a]

[a] *Department of Chemistry, University of Texas at San Antonio, One UTSA Circle, San Antonio, Texas 78249-0698, USA. Fax: (+1)-210-458-7428; E-mail: bin.li@utsa.edu; banglin.chen@utsa.edu*

[b] *Van 't Hoff Institute for Molecular Sciences, University of Amsterdam, Science Park 904, 1098 XH Amsterdam, The Netherlands*

1. General Procedures and Materials. All reagents and solvents were commercially available and used without further purification. 4,4′-diaminobiphenyl -3,3′,5,5′-tetrabromide was prepared according to the literature procedure.[1] ^{1}H NMR spectra were recorded on a Varian Mercury 500 MHz spectrometer using tetramethylsilane (TMS) as internal standards. The coupling constants reported in Hertz. FTIR spectra were performed on a Bruker Vector 22 spectrometer at room temperature. The elemental analyses were performed with Perkin–Elmer 240 CHN analyzers. Thermogravimetric analyses (TGA) were carried out using a Shimadzu TGA-50 analyzer under a nitrogen atmosphere with a heating rate of 5 ^{o}C min^{-1}. Powder X–ray diffraction (PXRD) patterns were measured by a Rigaku Ultima IV diffractometer operated at 40 kV and 44 mA with a scan rate of 1.0 deg min^{-1}.

2. Gas sorption Measurements. A Micromeritics ASAP 2020 surface area analyzer was used to measure gas adsorption isotherms. To remove all the guest solvents in the framework, the fresh sample of UTSA-67 was guest–exchanged with dry acetone at least 10 times, filtered and degassed at 273 K for 36 h, and then at 296 K for another 24 hours until the outgas rate was 5 μmHg min^{-1} prior to measurements. The sorption measurement was maintained at 77 K with liquid nitrogen. An ice-water bath (slush) and water bath were used for adsorption isotherms at 273 and 296 K, respectively.

3. Single-crystal X-ray crystallography. The crystal data were collected on an Agilent Supernova CCD diffractometer equipped with a graphite-monochromatic enhanced Cu Kα radiation (λ = 1.54184 Å) at 293 K. The datasets were corrected by empirical absorption correction using spherical harmonics, implemented in the SCALE3 ABSPACK scaling algorithm. The structure was solved by direct methods and refined by full matrix least-squares methods with the SHELX-97 program package.[2] The solvent molecules in the compound are highly disordered. The SQUEEZE subroutine of the PLATON software suit was used to remove the scattering from the highly disordered guest molecules.[3] The resulting new files were used to further refine the structures. The H atoms on C atoms were generated geometrically.

4. Fitting of pure component isotherms

Experimental data on pure component isotherms for C_2H_2, and C_2H_4 in UTSA-67a were measured at temperatures of 273 K and 296 K. The pure component isotherm data for C_2H_2, and C_2H_4 were fitted with the dual-Langmuir-Freundlich isotherm model

$$q = q_{A,sat}\frac{b_A p^{\nu_A}}{1+b_A p^{\nu_A}} + q_{B,sat}\frac{b_B p^{\nu_B}}{1+b_B p^{\nu_B}} \tag{1}$$

with T-dependent parameters b_A, and b_B

$$b_A = b_{A0}\exp\left(\frac{E_A}{RT}\right); \quad b_B = b_{B0}\exp\left(\frac{E_B}{RT}\right) \tag{2}$$

The fitted parameter values are presented in Table S2. The fits are excellent for both components over the entire pressure range.

5. Isosteric heat of adsorption

The isosteric heat of C_2H_2 adsorption, Q_{st}, defined as

$$Q_{st} = RT^2\left(\frac{\partial \ln p}{\partial T}\right)_q \tag{3}$$

was determined using the Clausius-Clapeyron equation by fitting the adsorption isotherms taken at 273 and 296 K to a Langmuir expression. Figure 4 presents a comparison of the heats of adsorption of C_2H_2 in UTSA-67a with five other representative MOFs. We note that values of Q_{st} in UTSA-67a, UTSA-100a and M'MOF-3a are significantly lower than that for MOFs with coordinately unsaturated metal atoms UTSA-60a,[4] FeMOF-74, CoMOF-74, and MgMOF-74. This implies that the regeneration energy requirement of M'MOF-3a, UTSA-67a, and UTSA-100a will be significantly lower than that of UTSA-60, FeMOF-74, CoMOF-74, and MgMOF-74.

6. IAST calculations of adsorption selectivities

The selectivity of preferential adsorption of component *1* over component *2* in a mixture containing *1* and *2*, can be formally defined as

$$S_{ads} = \frac{q_1/q_2}{p_1/p_2} \tag{4}$$

In equation (4), q_1 and q_2 are the absolute component loadings of the adsorbed phase in the mixture. These component loadings are also termed the uptake capacities. We calculate the values of q_1 and q_2 using the Ideal Adsorbed Solution Theory (IAST) of Myers and Prausnitz.[5]

Based on the IAST calculations for C_2H_2/C_2H_4 adsorption selectivities, at a total pressure of 100 kPa, the value of S_{ads} for UTSA-67a is in the range of 5–6, which is comparable to UTSA-100a and UTSA-60a,[4] but much higher than that for NOTT-300 (2.17)[5] and MMOF-74 (in the range of 1.6 to 2.2).

7. Transient breakthrough of C_2H_2/C_2H_4 mixtures in fixed bed adsorbers

The performance of industrial fixed bed adsorbers is dictated by a combination of adsorption selectivity and uptake capacity. For a proper comparison of various MOFs, we perform transient breakthrough simulations using the simulation methodology described in the literature.[6-8] For the breakthrough simulations, the following parameter values were used: framework density, ρ = 1057 kg m^{-3}, length of packed bed, L = 0.12 m; voidage of packed bed, ε = 0.75; superficial gas velocity at inlet, u = 0.00225 m/s. The transient breakthrough simulation results are presented in terms of a *dimensionless* time, τ, defined by dividing the actual time, t, by the characteristic time, $\frac{L\varepsilon}{u}$.

The transient breakthrough simulations in Figure 3b show the concentrations of C_2H_2/C_2H_4 exiting the adsorber packed with UTSA-67a as a function of the dimensionless time, τ. Analogous breakthrough simulations were performed for UTSA-100a, MgMOF-74, FeMOF-74, CoMOF-74, and M'MOF-3a using the isotherm fits parameters that are provided in our earlier work.[8] On the basis of the gas phase concentrations, we can calculate the impurity

level of C_2H_2 in the gas mixture exiting the fixed bed packed with five different MOFs. Figure S10 shows the ppm C_2H_2 in the outlet gas mixture exiting an adsorber packed with UTSA-67a, UTSA-100a, MgMOF-74, FeMOF-74, CoMOF-74, and M'MOF-3a. At a certain time, τ_{break}, the impurity level will exceed the desired purity level of 40 ppm (indicated by the dashed line), that corresponds to the purity requirement of the feed to the polymerization reactor. The adsorption cycle needs to be terminated at that time τ_{break} and the regeneration process needs to be initiated. From a material balance on the adsorber, the amount of C_2H_2 captured during the time interval $0-\tau_{break}$ can be determined. Table 2 provides a summary of the breakthrough times, τ_{break} for various MOFs and the amount of C_2H_2 captured, expressed in mmol per L adsorbent in fixed bed

Figure S11 presents a plot of the amount of C_2H_2 captured plotted as a function of the time interval τ_{break}. The hierarchy of C_2H_2 capture capacities is UTSA-100a > MMOF-74 > UTSA-67a > M'MOF-3a > NOTT-300 > UTSA-60a (Table S4).

Notation

b_A	dual-Langmuir-Freundlich constant for species *i* at adsorption site A, $Pa^{-\nu_i}$
b_B	dual-Langmuir-Freundlich constant for species *i* at adsorption site B, $Pa^{-\nu_i}$
L	length of packed bed adsorber, m
p_i	partial pressure of species *i* in mixture, Pa
p_t	total system pressure, Pa
q_i	component molar loading of species *i*, mol kg^{-1}
q_t	total molar loading in mixture, mol kg^{-1}
q_{sat}	saturation loading, mol kg^{-1}
Q_{st}	isosteric heat of adsorption, J $kmol^{-1}$
t	time, s
T	absolute temperature, K
u	superficial gas velocity in packed bed, m s^{-1}

Greek letters

ε	voidage of packed bed, dimensionless
ν	exponent in dual-Langmuir-Freundlich isotherm, dimensionless
ρ	framework density, kg m^{-3}
τ	time, dimensionless

Subscripts

i	referring to component i
t	referring to total mixture

Scheme S1. Synthetic routes to the organic linker H_4L.

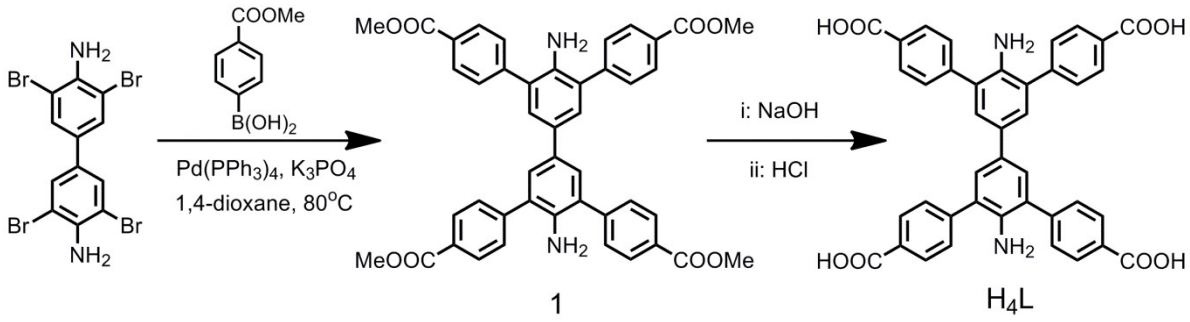

Synthesis of 4,4′-diaminobiphenyl-3,3′,5,5′-tetra-(phenyl-4-carboxylic acid) (H_4L): A mixture of 4,4′-diaminobiphenyl -3,3′,5,5′-tetrabromide (2.48 g, 5 mmol) and 4-methoxycarbonylphenylboronic acid (3.96 g, 22 mmol) were dissolved in dry 1,4-dioxane (80 mL), which was deoxygenated by three freeze-pump-thaw cycles and then protected under N_2 atmosphere. After that, K_3PO_4 (2.55g, 12 mmol) and [$Pd(PPh_3)_4$] (0.3 g, 0.26 mmol) were quickly added to the reaction mixture with stirring and the mixture was heated to 85 ^oC for two days. After cooling down to room temperature, compound 1 was isolated by conventional extraction and procedures. The final product H_4L was obtained by hydrolysis of compound 1 with 2M aqueous NaOH, followed by acidification with concentrated HCl.

Yield: 1.5 g (46%). ^{1}H NMR (500 MHz, d^{6}-DMSO, ppm): δ = 8.04 (d, *J* = 8.10 Hz, 8H), 8.01 (d, *J* = 8.0 Hz, 8H), 7.64 (s, 4H), 6.61 (s, 4H). ^{13}C NMR (d^{6}-DMSO, ppm): δ = 167.61, 143.13, 131.66, 130.46, 130.28, 130.21, 128.92.

Synthesis of UTSA-67. A mixture of the organic linker H_4L (10.0 mg, 0.015 mmol) and $Zn(NO_3)_2{\cdot}6H_2O$ (25.0 mg, 0.084 mmol) was dissolved into a 2.4 mL mixed solvent (DMF/EtOH, 2 mL/0.4 mL) in a screw-capped vial (20 mL). The vial was capped and heated in an oven at 80 °C for 24 h. Dark yellow crystals were obtained by filtration and washed with DMF several times to afford UTSA-67 in 60% yield. UTSA-67 has a best formula as $[Zn_2L]{\cdot}2DMF{\cdot}4H_2O$, which was obtained based on the basis of single-crystal X-ray structure determination, elemental analysis and TGA. Anal. Calcd for $C_{48}H_{50}N_4O_{14}Zn_2$: C, 55.56; H, 4.86; N, 5.40; found: C, 55.37; H, 4.88; N, 5.45. TGA data for loss of 2DMF and $4H_2O$: calcd: 23.80%, found: 23.75%.

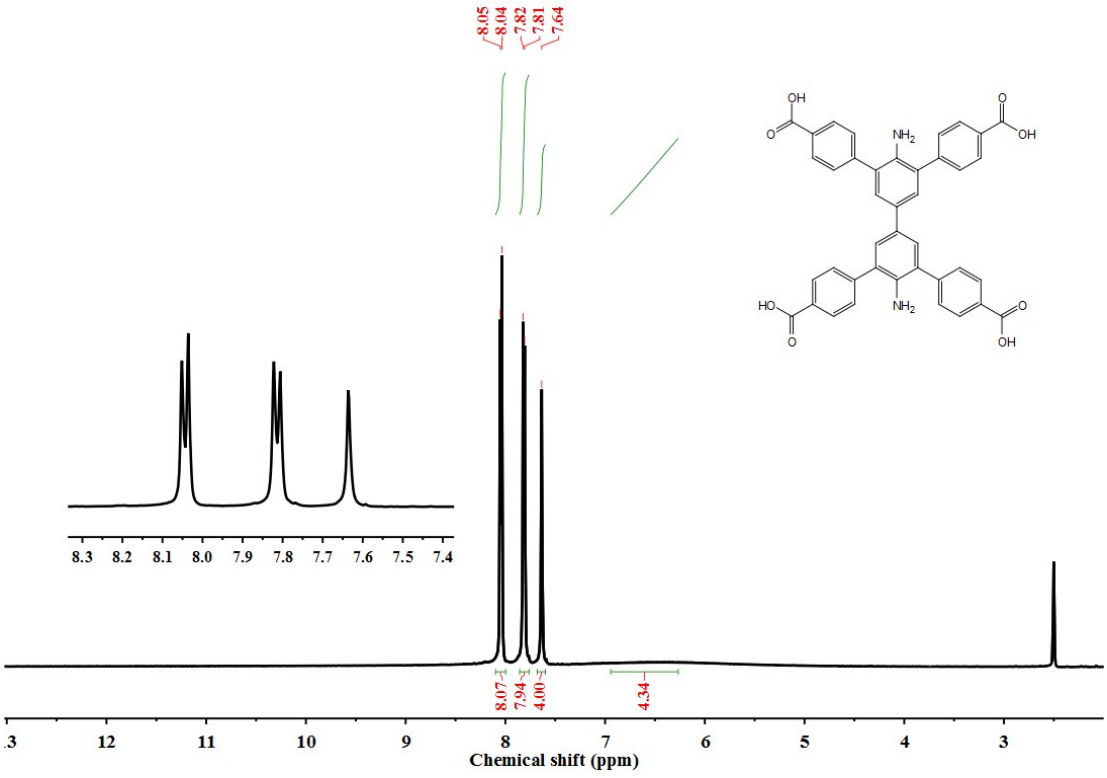

Figure S1. ^{1}H (DMSO-d$_6$, 500MHz) spectra of the ligand H_4L.

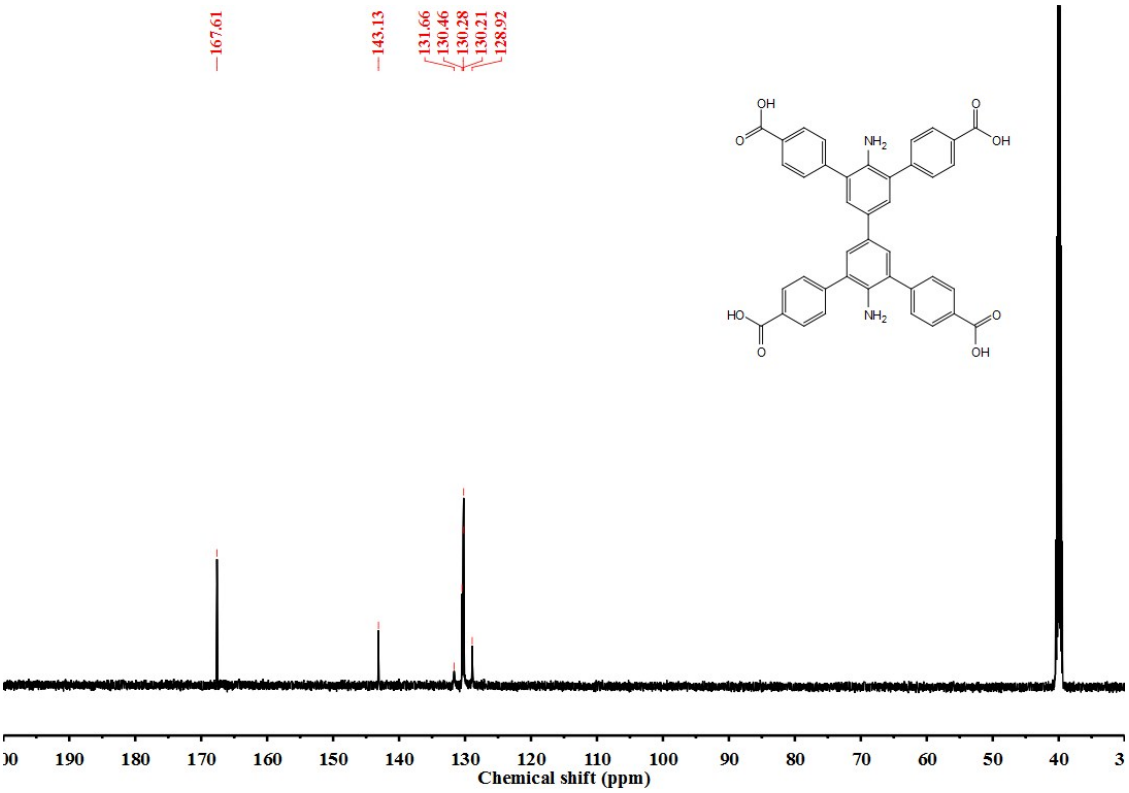

Figure S2. ^{13}C (DMSO-d_6, 500MHz) spectra of the ligand H_4L.

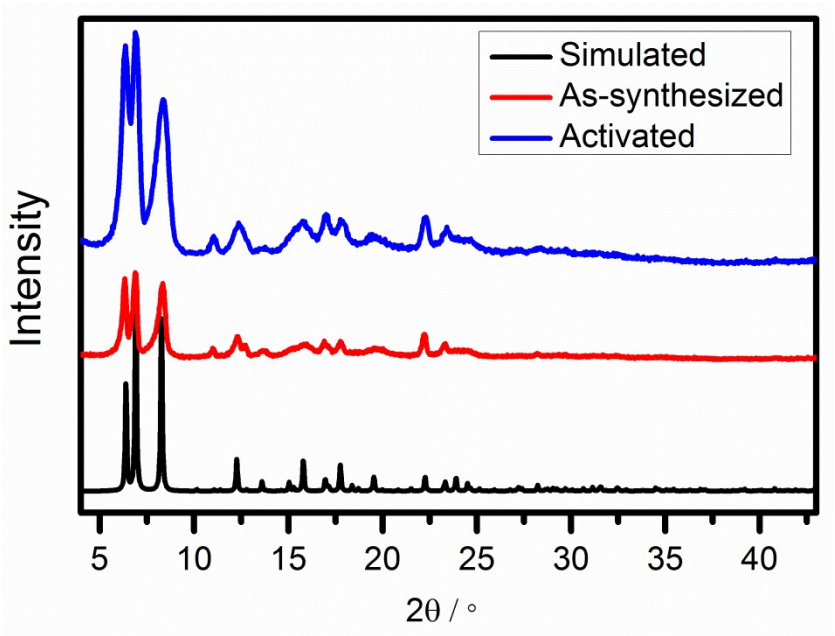

Figure S3. PXRD patterns of as-synthesized UTSA-67 (red) and activated UTSA-67a (blue) along with the simulated XRD pattern from the single-crystal X-ray structure (black).

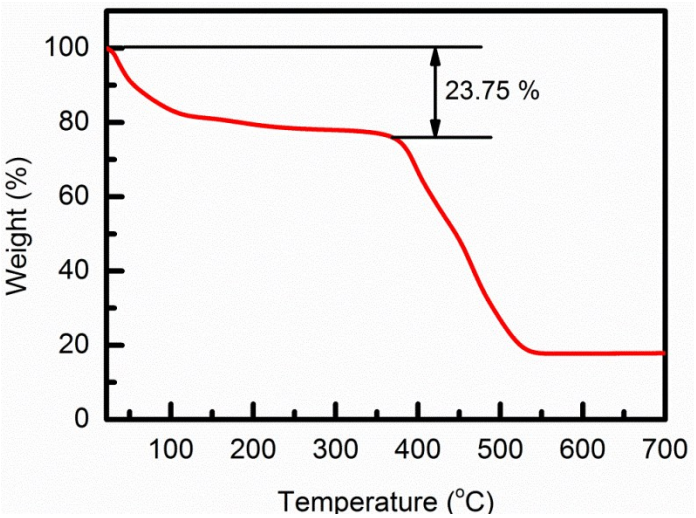

Figure S4. TGA curves of as–synthesized UTSA-67.

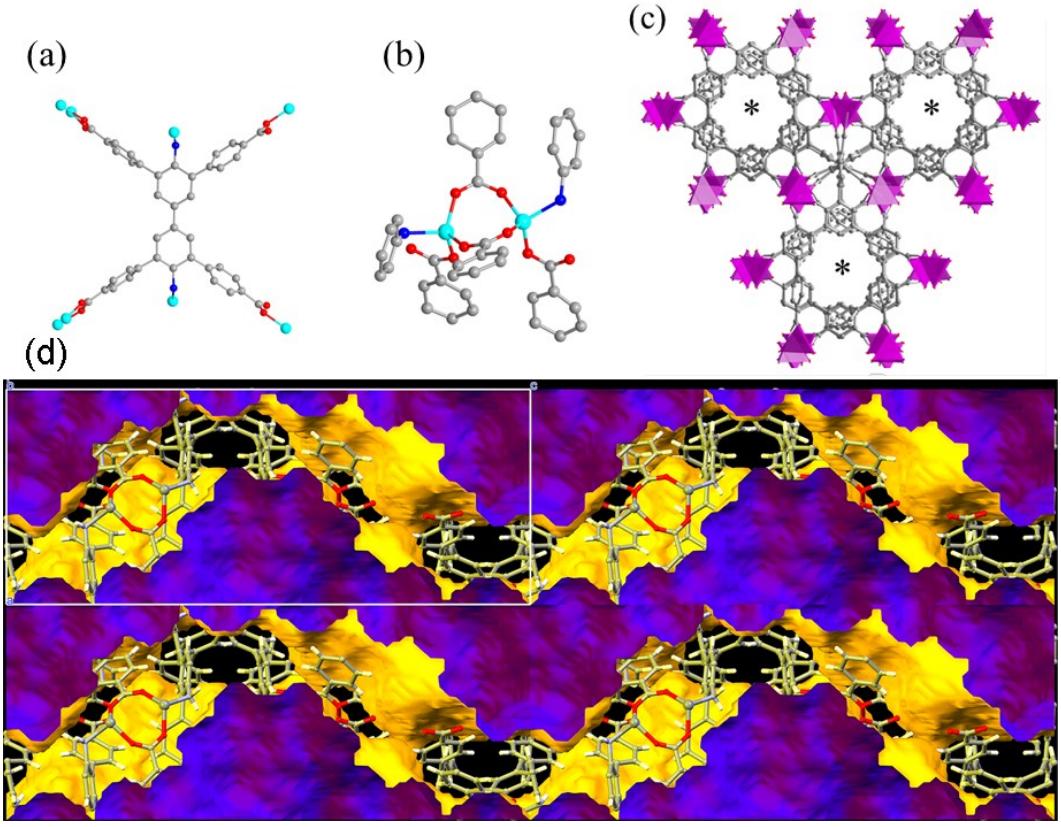

Figure S5. X-ray single crystal structure of UTSA-67: (a) coordination modes of carboxylate and amino groups in the organic linker; (b) the coordination environment of the binuclear zinc cluster; (c) the pore channels viewed along the *c* axes. The symbols of * represent the 6-fold screw axes. (d) the one-dimensional channel along the *c* axes.

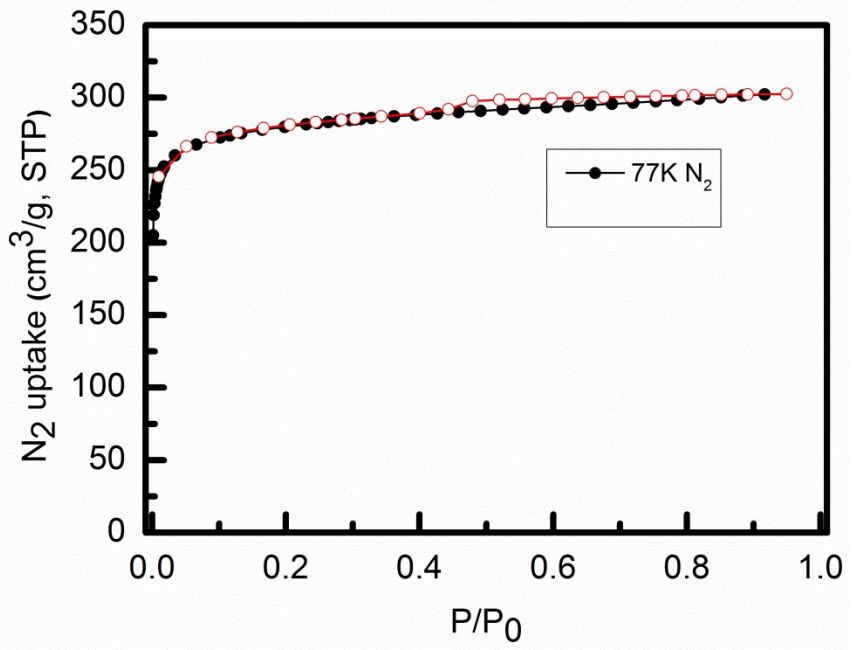

Figure S6. N_2 sorption isotherms of UTSA-67a at 77 K. Closed symbols, adsorption; open symbols, desorption.

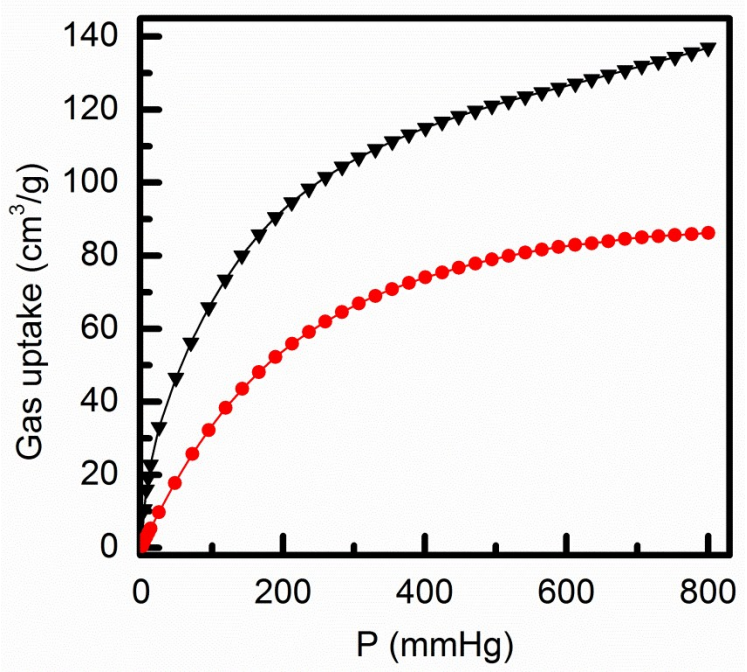

Figure S7. Single-component adsorption isotherms for C_2H_2 (black) and C_2H_4 (red) of UTSA-67a at 273 K.

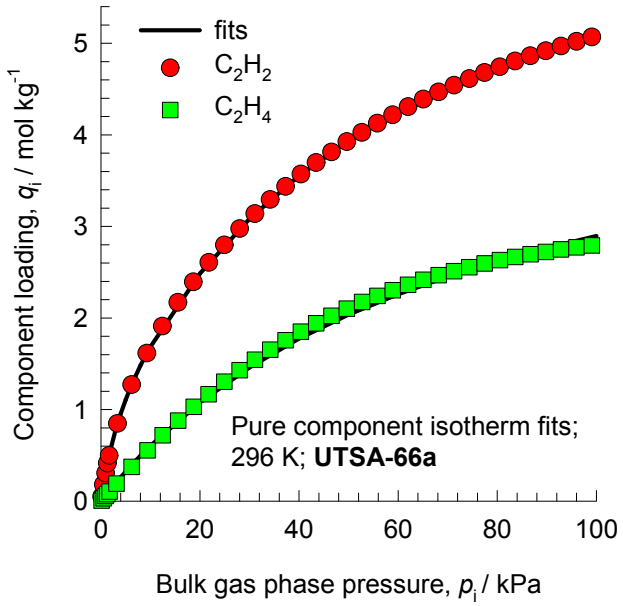

Figure S8. Comparison of component loadings for C_2H_2, and C_2H_4 at 296 K in UTSA-67a with the dual-Langmuir-Freundlich isotherm fits.

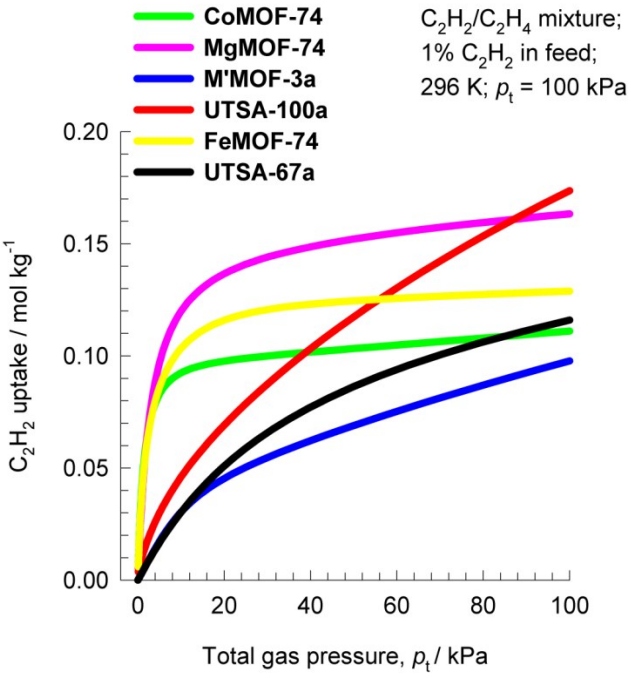

Figure S9. IAST calculations of the uptake capacity of C_2H_2 for adsorption from C_2H_2/C_2H_4 mixtures containing 1% C_2H_2. The partial pressures of C_2H_2, and C_2H_4 are, respectively, p_1 = 1 kPa, p_2 = 99 kPa at T = 296 K. The data for FeMOF-74 is at a temperature of 318 K; this is the lowest temperature used in the isotherm measurements of Bloch et al.[9]

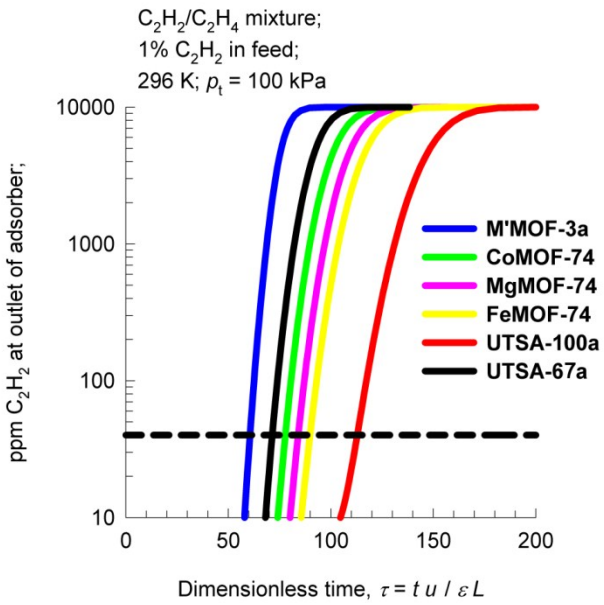

Figure S10. Ppm C_2H_2 in the outlet gas of an adsorber bed packed with UTSA-67a, MgMOF-74, CoMOF-74, FeMOF-74, M'MOF-3a, and UTSA-100a. The total bulk gas phase is 100 kPa; the partial pressures of C_2H_2, and C_2H_4 in the inlet feed gas mixture are, respectively, p_1 = 1 kPa, p_2 = 99 kPa. The temperature is 296 K for all MOFs except FeMOF-74 for which the chosen temperature is 318 K.[9]

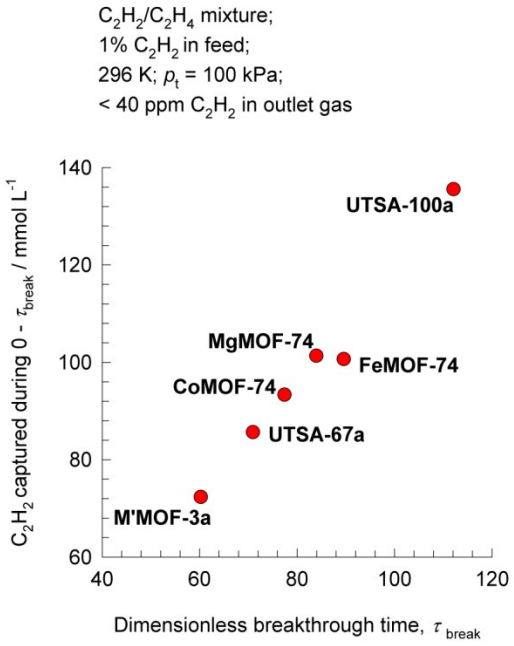

Figure S11. Plot of C_2H_2 captured per L of adsorbent, during the time interval $0-\tau_{break}$, plotted as a function of the time interval τ_{break}. The temperature is 296 K for all MOFs except for FeMOF-74 for which the chosen temperature is 318 K.

Table S1. Crystallographic data and structure refinement results for UTSA-67 (from single-crystal X-ray diffraction analysis on the as-synthesized sample).

	UTSA-67
Formula	$C_{40}H_{24}N_2Zn_2O_{11}$
Formula weight	839.39
Temperature/K	293.00(19)
Crystal system	hexagonal
Space group	P6522
a (Å)	15.9684(5)
b (Å)	15.9684(5)
c (Å)	33.649(4)
α (°)	90.00
β (°)	90.00
γ (°)	120.00
V (Å^3)	7430.6(9)
Z	12
D_{calcd} (g cm^{-3})	1.0572
μ (mm^{-1})	1.017
F(000)	2556.0
Crystal size/mm^3	0.30 × 0.20 × 0.20
GOF	1.070
R_{int}	0.0816
R_1, wR_2 [I>=2σ (I)]	0.1139, 0.2978
R_1, wR_2 [all data]	0.1616, 0.3341
Largest diff. peak and hole (e Å^{-3})	0.874, -0.675

Table S2. Dual-Langmuir-Freundlich parameter fits for UTSA-67a.

	Site A				Site B			
	$q_{A,sat}$ mol kg^{-1}	b_{A0} $Pa^{-\nu_i}$	E_A kJ mol^{-1}	ν_A dimensionless	$q_{B,sat}$ mol kg^{-1}	b_{B0} $Pa^{-\nu_i}$	E_B kJ mol^{-1}	ν_B dimensionless
C_2H_2	1.7	3.07×10^{-10}	33	1.25	5.2	5.46×10^{-11}	25	1
C_2H_4	5	2.56×10^{-10}	26.8	1				

Table S3. Comparison of some microporous MOFs for C_2H_2/C_2H_4 separation at room temperature.

	UTSA-67a	M'MOF-3a	CoMOF-74	MgMOF-74	FeMOF-74	NOTT-300	UTSA-100a	UTSA-60a
Surface area ($m^2\ g^{-1}$)[a]	1136.7	110	1018	927	1350	1370	970	484
Pore volume ($cm^3\ g^{-1}$)	0.47	0.165	0.515	0.607	0.626	0.433	0.399	0.189
Size of pore window (Å)	3.3×3.3	3.4×4.8	11×11	11×11	11×11	6.5×6.5	4.3×4.3	4.8×4.0
C_2H_2 uptake (mmol g^{-1})	5.13	1.90	8.17	8.37	6.80[b]	6.34[c]	4.27	3.12
C_2H_4 uptake (mmol g^{-1})	2.81	0.40	7.02	7.45	6.10[b]	4.28[c]	1.66	2.05
C_2H_2/C_2H_4 uptake ratio	1.84	4.75	1.16	1.12	1.11	1.48	2.57	1.52
Selectivity[d]	5–6	24.03	1.70	2.18	2.08	2.17	5–10.7	5.5–16
Q_{st} (C_2H_2, kJ mol^{-1})[e]	32	25	45	41	46	32	22	36
Ref.	This work	8	8	8	9	5	5	4

[a] BET. [b] At temperature of 318 K. [c] At temperature of 293 K. [d] IAST analysis for C_2H_2/C_2H_4 mixtures containing 1% acetylene at 100 kPa. [e] The initial Q_{st} values.

Table 4. Breakthrough calculations for separation of C_2H_2/C_2H_4 mixture containing 1 mol% C_2H_2 at 296 K. The data for FeMOF-74 is at a temperature of 318 K; this is the lowest temperature used in the isotherm measurements of Bloch et al.[9] The product gas stream contains less than 40 ppm C_2H_2.

MOFs	Dimensionless breakthrough time τ_{break}	C_2H_2 adsorbed during 0 - τ_{break} mmol L^{-1}	Ref.
CoMOF-74	77.4	93.3	8
MgMOF-74	84	101.3	8
FeMOF-74	89.6	100.7	8
UTSA-100a	112	135.5	5
M'MOF-3a	60.2	72.3	8
NOTT-300	56.2	68.3	5
UTSA-60a	55	52	4
UTSA-67a	70.9	85.7	This work

References

1. Wehrmann, P. and Mecking S., *Organometallics*, 2008, **27**, 1399–1408.

2. Sheldrick, G. M. Program for Structure Refinement. Germany, **1997**.

3. Spek, L. PLATON: The University of Utrecht: Utrecht, The Netherlands, **1999**.

4. H.-M. Wen, B. Li, H. Wang, C. Wu, K. Alfooty, R. Krishnad and B. Chen, *Chem. Commun.*, 2015, **51**, 5610–5613.

4. A. L. Myers and J. M. Prausnitz, *A.I.Ch.E.J.*, 1965, **11**, 121–127.

5. T.-L. Hu, H. Wang, B. Li, R. Krishna, H. Wu, W. Zhou, Y. Zhao, Y. Han, X. Wang, W. Zhu, Z. Yao, S. Xiang and B. Chen, *Nat. Commun.*, 2015, **6**, 7328.

6. R. Krishna and J. R. Long, *J. Phys. Chem. C*, 2011, **115**, 12941–12950.

7. R. Krishna, *Microporous Mesoporous Mater.*, 2014, **185**, 30–50.

8. Y. He, R. Krishna and B. Chen, *Energy Environ. Sci.*, 2012, **5**, 9107–9120.

9. E. D. Bloch, W. L. Queen, R. Krishna, J. M. Zadrozny, C. M. Brown and J. R. Long, *Science*, 2012, **335**, 1606–1610.